**Orientation and swimming mechanics by the scyphomedusa *Aurelia* sp. in shear flow**

Kelly C. Rakow[1] and William M. Graham

Dauphin Island Sea Lab, Dauphin Island, Alabama 36528, and Department of Marine Sciences, University of South Alabama, Mobile, Alabama 36888

[1] Present address: Woods Hole Oceanographic Institution, Woods Hole, Massachusetts 02543 (krakow@whoi.edu)

Running title: Swimming mechanics of scyphomedusae

Acknowledgements

We thank the crew of the RV *Pelican* for field assistance. We are grateful to H. Fletcher, J. Higgins, D. Martin, and J. Martin for technical support and thoughtful discussions. Input from K. Park and J. Costello substantially improved the quality of this work. The research was supported by the National Science Foundation (OCE 9733441).

Abstract

Individual *Aurelia* sp. medusae were distributed around regions of current shear associated with vertical density discontinuities during three vertically towed camera profiles in the northern Gulf of Mexico. Along shear regions, medusae oriented non-randomly and swam horizontally, forming distinct layers. To identify the mechanisms by which *Aurelia* maintain horizontal orientation in velocity shear, jellyfish swimming mechanics were studied in laboratory kreisel tanks at three shear rates (0.10, 0.21, and 0.34 $s^{-1}$) and a no flow control. Medusae counteracted the rotational effect of velocity shear by pulsing asymmetrically. Specifically, medusae held a position against shear flow by maintaining a higher bell margin angle on the side of the medusa in higher flow velocity. Swimming asymmetry increased with shear and, as a result, the ratio between bell angles on opposing flow sides was significantly different from the control at all shear rates. Contractions were initiated on the lower flow side of the bell in all cases and at the highest shear rate, the low flow side of the bell contracted 0.2 s before the high flow side. Laboratory observations confirm that patches of jellyfish at vertical discontinuities may be the result of an active behavioral response to vertical velocity shear. Layers of jellyfish formed via an active behavioral response to shear may improve prey encounter or fertilization success.

## Introduction

Aggregations of scyphomedusae result from the interplay between sensory physiology and behavior of medusae and their physical, chemical, and biogeochemical surroundings (reviewed by Graham et al. 2001). Prior investigations have suggested that medusae are passively accumulated by buoyancy, along density gradients (Nielson et al. 1997), or by currents (Sparks et al. 2001). While physics undoubtedly plays a role in passively aggregating medusae, active behavioral responses are usually required to provide a mechanism for accumulation (reviewed by Graham et al. 2001). Previous in situ studies have documented that medusae orient to flow features such as pycnoclines (Graham et al. 2003b), tidal currents (Costello et al. 1998), wind-driven currents (Shanks and Graham 1987), fronts (Graham 1994), and Langmuir convergences (Hamner and Schneider 1986) but with the exception of Graham et al. (2003b), these studies did not include velocity measurements along with orientation data. While fluid motion occurs over a range of spatial scales, medusae interact with fluid features from the diameter of the medusa (10s of cm) to the medusa's realm (100s of meters). Mobile organisms can aggregate any time they swim fast enough to overcome advection out of an area (Mackas et al. 1985) or when swimming counteracts the rotational force created by a velocity gradient (Tiselius et al. 1994).

Cnidarians have a simple, diploblastic body plan and lack a central nervous system, yet based on their phylogenetic position, there is no reason to assume that cnidarians are unsophisticated organisms (Mackie 1999). Radial symmetry allows for multiple sensory structures situated in rhopalia around the bell margin (Fig. 1). The statocyst and touch plate, a group of sensory cells, located in the rhopalium are the structures responsible for sensing gravity (Hüngden and Biela 1982). Although individual statocysts are incapable of detecting the

direction of a stimulus, this limitation might be overcome by the presence of multiple sensory organs around the bell margin (Fig. 1B; Budelmann 1988).

With the use of these balancing organs, scyphomedusae are capable of maintaining an orientation and can compensate when they are steered off course (Shanks and Graham 1987). Turning, like orientation, is a response to an environmental stimulus. Scyphozoans are able to turn by pulsing asymmetrically (Gladfelter 1972). First one side contracts, tilting the animal sideways. After a delay, the second side (i.e. the outboard side) contracts but the magnitude of contraction is enhanced compared to the leading side, and a turn is effected.

It is critical to understand relationships between swimming mechanics and jellyfish aggregation, since directional swimming often plays a role in swarm formation. Ultimately, aggregations of medusae can have profound ecological and socio-economic impacts. Recent evidence of distributional and seasonal range expansions, numerical increases, and anthropogenic introductions of gelatinous zooplankton (Graham 2001; Sullivan et al. 2001; Graham et al. 2003a) has underscored the key ecological role of these predators in a wide range of ecosystems. In addition, gelatinous predators are capable of feeding on fish eggs and larvae, leading to decreases in commercial fisheries stocks (Cowan and Houde 1993; Purcell and Arai 2001).

Jellyfish aggregations are often associated with physical features in marine environments; yet, there is no direct evidence that scyphomedusae respond to fluid flow, and the behavioral mechanism by which a medusa maintains a position into a current has never been investigated. In this study, we explored the orientation and swimming mechanics of the jellyfish *Aurelia* sp. The following questions were addressed: (1) Do scyphomedusae orient to velocity shear and, if so, (2) what is the behavioral mechanism for orienting to shear?

Materials and methods

*Field observations*- Three JellyCam video profiles of *Aurelia* sp. patches were collected in the northern Gulf of Mexico on 13, 18, and 20 August 2000 from the 32-m RV *Pelican*. The JellyCam is a towed video system used for in situ quantification and observation of large medusae in conjunction with real time CTD and Digital GPS data (Graham et al. 2003b). The camera was lowered vertically in 2-m increments and towed horizontally at a speed of 1 m $s^{-1}$ for 1 min at each depth. For all data analyses, the water column was divided into 2-m depth bins and the number of medusae per cubic meter of water was calculated. Medusae were assigned a heading angle in 45˚ increments between 0˚ (aboral side up) and 180˚ (aboral side down). At depths where more than 5 medusae were observed, Rayleigh's test was used to determine if *Aurelia* sp. were randomly or directionally oriented (Batchelet 1981).

Current velocity measurements were taken with a vessel-mounted, narrowband 600 kHz ADCP (RD Instruments) during or immediately after the JellyCam tow. Mean current velocity and standard error were calculated in 2-m depth bins by averaging velocity measurements taken over a 1-min interval with 1-m resolution.

*Laboratory observations*- Behavioral observations of *Aurelia* sp.were made at three velocity shear rates and a no flow control, based on the range of shear experienced by medusae in situ as measured above, below, and at the halocline from the northern Gulf of Mexico during July and August 2002 (Higgins 2005). Experimental observations were made in modified kreisel tanks (100 x 75 x 40 cm) characterized by circular flow, which keeps gelatinous plankton suspended and free of the intake and tank walls (Hamner 1990; Raskoff et al. 2003).

*Aurelia* sp. medusae between 15 and 25 cm in diameter were collected with dip nets from the northern Gulf of Mexico during August and September 2003. Medusae were maintained in

pseudokreisel tanks, and observations were made within one week of collection. Medusae were fed *Artemia* nauplii or thawed Cyclop-eeze copepods 1-2 times daily. Tank temperature ranged from 23°C to 26°C and salinity ranged from 25 to 35, closely matching the environmental conditions at the time of collection.

Current velocity in the kreisel tank was characterized by acoustic Doppler velocimeter (ADV) measurements (SonTek, emission frequency = 10 MHz; sampling rate = 210 Hz) at 5-cm intervals. *Artemia* cysts were used as ambient particles to reflect acoustic beams back to the receiver. Three replicate velocity measurements taken for 30-s periods at each grid node were processed using WinADV32 (developed by T.L. Wahl, U.S. Bureau of Reclamation). The mean velocity at each grid node was used to establish the shear rate in the pseudokreisel and was visually represented with vector plots plotted in Surfer 8 (Golden Software, Inc.). Shear rate (D) is described by the following equation:

$$D = \frac{\partial \mathrm{w}}{\partial \mathrm{x}} \tag{1}$$

where **w** is the water velocity in the vertical direction and **x** is distance in the horizontal direction.

Behavior was recorded in two dimensions using a digital video camera (Sony MiniDV). At each treatment level, ten individual medusae were videotaped for 20 minutes. A black background with 5-$cm^2$ white gridlines placed behind the tank provided scale for video analysis. The video camera remained stationary on an observational window on one side of the tank. Prior to each observation, a pin was inserted at the top of the bell to serve as a landmark for swimming measurements (Fig. 1A). Preliminary observations conducted with and without a pin indicated that insertion of a pin in the bell did not influence swimming behavior.

The swimming movements of medusae were quantified by comparing the range of the bell margin angle on either side of the medusa. This bell margin angle was approximated by drawing a central oral-aboral axis, using the pin inserted at the top of the bell as a landmark, and drawing a second line from the top of the bell to the edge of the bell to create a measurable angle (Fig. 1A). The margin angles on each side of the bell were measured over a pulse sequence to indicate whether the animal was pulsing non-uniformly. For each 20-minute jellyfish observation, three swimming sequences (3-5 pulse cycles) were analyzed at 0.1-s intervals. Bell margin angles were reported as "high flow" and "low flow" bell margin angle in all treatments including the control.

To test the hypothesis that bell pulsation is symmetrical, the mean bell angle was compared between the two sides of the medusae using two-sample *t*-tests performed using Minitab 13.1. The ratio of the mean bell angle corresponding to the lower flow side ($\Phi_l$) to the mean bell angle corresponding to the higher flow side ($\Phi_h$) was calculated and compared to 1:1 ratio to detect a departure from symmetry. These ratios were then analyzed for treatment effects with a one-way ANOVA and a post-hoc Tukey test for multiple comparisons (Minitab 13.1). The use of ratios provides a way to standardize and compare swimming across treatments but ratio data poses limitations for statistical analysis because the relationship between the numerator and denominator is masked, so conclusions should be interpreted somewhat cautiously (Liermann et al. 2004).

Results

In situ *vertical distribution* - The water column was stratified on 13 August with pronounced velocity shear between 2 and 4 m and again between 12 and 14 m (Fig. 2A). Most medusae were distributed in the region of velocity shear near the sea floor (Fig. 2B). At this depth, the medusae were swimming horizontally at a mean angle of 85.12˚ (Fig. 2C) and were non-randomly distributed (Rayleigh's *z*, $p<0.001$).

On 18 August, a marked surface layer to 8 m depth was characterized by a weak density gradient. A pronounced pycnocline was located between 15 and 17 m, however, the region of highest velocity shear was above the pycnocline between 12 and 14 m (Fig. 3A). Velocity shear was also present in the upper layer of the water column, below the pycnocline and above the benthic boundary layer. *Aurelia* sp. were mostly concentrated (72%) between 14 and 18 m below the pycnocline with a single maximum between 16 and 18 m (Fig. 3B). Medusae were non-randomly oriented in the horizontal direction (Rayleigh's *z*, $p<0.001$; Fig. 3C).

The JellyCam profile conducted on 20 August was in 144 m of water off the continental shelf, although the camera was only lowered to a depth of 54 m (Fig. 4). The water column was highly structured (Fig. 4A), and a velocity gradient was pronounced from the surface to 16 m depth. A single pycnocline was located between 14 and 20 m (Fig. 4A). Highest numbers of *Aurelia* sp. were located above 10 m where velocity shear was most pronounced (Fig. 4B). Medusae within this region were primarily swimming in the horizontal direction, between 45˚ and 135˚ (Fig. 4C). In the upper 6 m of the water column where shearing was greatest, the swimming mode was at 90˚ or angled slightly up. A second strong region of shear was located at 10 m. Between 6 and 10 m, medusae were swimming downward.

*Laboratory swimming mechanics* – The rotational motion of water in the kreisel created flow velocity gradients across the tank. Flow velocities and shear rates were most pronounced at the kreisel boundary and lowest toward the center of the tank (Fig. 5). Horizontal profiles of velocity and shear were used to describe the flow field (Table 1; Fig. 6). Maximum velocity ranged from 3.02 (± 0.28) cm $s^{-1}$ in the low flow treatment to 10.21 (± 0.05) cm $s^{-1}$ in the high flow treatment. The three flow treatments produced shear rates of 0.10 $s^{-1}$, 0.21 $s^{-1}$, and 0.34 $s^{-1}$, respectively.

Medusa bell contraction was symmetrical in the no flow treatment and increasingly asymmetrical as velocity shear increased. Figure 7 depicts a sequence of images of an individual *Aurelia* sp. medusa swimming in shear flow showing the difference in bell angle on the two sides of the medusa. The relative magnitude of bell contraction between the two sides of the bell increased in the presence of highest shear (0.34 $s^{-1}$) compared to the control (Fig. 8A and B). At the highest velocity shear (0.34 $s^{-1}$) the mean bell margin angle was higher on the high velocity side of the experimental tank than on the low flow side (two-sample *t*-test, $p = 0.05$; Table 2). However, in the low (0.10 $s^{-1}$) and medium (0.21 $s^{-1}$) shear treatment, low and high flow bell margin angles were not significantly different from the control bell margin angles (two-sample *t*-test, $p>0.05$; Table 2).

The ratio of bell margin angles in the no flow treatment was significantly different from the ratios in the other three flow treatments (ANOVA, Tukey test, $p<0.05$; Table 4; Fig. 9). The ratio in the no flow treatment was greater than one while the ratios in shear treatments were all less than one.

*Data fitting* - Additional information about the kinematics of jellyfish swimming was produced by fitting raw data for each swimming sequence with the following four parameter sine equation using SigmaPlot 8.0 (SPSS, Inc.)

$$y = y_o + a \sin \frac{2\pi}{b}(t + c) \tag{2}$$

where $y_o$ is the height of the baseline or average angle (rad), $a$ is the amplitude (rad), $t$ is time (s), $b$ is period (s) and $c$ is phase shift or temporal offset (s).

For each fitted curve, parameter coefficients of $y_o$, $a$, $b$ and $c$, standard errors and $R^2$ with associated $p$-values were generated (Fig. 10). Parameter coefficients, $y_o$ and $a$ (units of radians), for the two sides of the bell were then compared within treatments using a paired Watson-Williams test. Parameter coefficients $b$ and $c$ (units of s) for the two sides of the bell were compared within treatments using $t$-tests.

The four-parameter sine curve approximated the raw data successfully ($R^2$ = 0.25 to 0.94, mean 0.70, ANOVA, $p< 0.01$). There were no significant differences between contraction period, phase shift, and bell margin amplitude across the two sides of medusae in any of the flow treatments (two-sample $t$-test, $p>0.05$). However, the mean bell margin angle was different at the highest shear rate treatment of 0.34 $s^{-1}$ (two-sample $t$-test, $p<0.05$; Table 3). There was a pattern of increasing difference in phase shift with increasing shear (Table 4). At all shear rates, the larger phase shift was associated with the low flow side of the bell, indicating that contractions were initiated on the low flow side of the bell. At the highest shear rate, the low flow side of the bell contracted 0.2 s before the high flow side.

A typical equation solution for the two sides of the bell was generated for each flow treatment by averaging the equation parameters, $a$, $b$, $c$, and $y_o$ (Table 3). Equation solutions for the shear treatments show a 1:1 relationship in the no flow control and an increasing divergence

in mean angle, $y_0$, with increasing shear flow (Fig 12A-D). Consequently, the ratio of $y_o$ on the low flow side of the bell to $y_o$ on the high flow side of the bell deviated from a 1:1 ratio with increasing shear velocity (Fig. 11E- H). The average angle ratio oscillated as the medusa swam, with the lowest ratio values (i.e., largest asymmetry between the two sides of the medusa) occurring just before the time of maximum contraction on the low flow side of the bell. The contraction period and amplitude, however, were the same on the two sides of the bell at all shear treatments (two-sample *t*-test, $p>0.05$).

Discussion

Field observations indicate that local populations of *Aurelia* sp. in the northern Gulf of Mexico orient horizontally in regions associated with vertical velocity shear (Figs. 2-4). The proximate cue for orientation is not completely clear, as medusae were most concentrated either above (Figs. 3B, 4B) or within (Fig. 2B) regions of pronounced shearing but also occurred below regions of shearing (Figs. 3B, 4B). In general, medusae associated with shear features maintained a 90° heading (Figs. 2C, 3C, 4C). Medusae located between two regions of shearing on 20 August may have orienting to the closest shear feature. *Aurelia* sp. located below a region of pronounced shearing at 4 m were swimming upward at 50° and medusae above a region of pronounced shearing at 10 m were swimming downward at 128° (Fig. 4C). Precise behavioral inferences are not possible, as density and velocity profiles varied in the field (Figs. 2A, 3A, 4A).

Laboratory observations confirmed that *Aurelia* sp. orient directionally against shear and showed that they accomplish oriented swimming by pulsing asymmetrically. Medusae maintain a higher bell margin angle on the side of the bell in higher flow velocity throughout a pulse cycle (Tables 2, 3; Figs. 7, 8, 11). A pulse is initiated on the lower flow side of the bell and the second side contracts after a delay. (Table 4, Figs. 7, 11). These swimming movements result in an increasing asymmetry between the two sides of the bell in increasing levels of shear (Fig. 9).

The distribution of plankton with respect to hydrographic features is well studied, but until recently, very few investigations have included hydrodynamic features such as turbulence and shear. At large spatial scales (10s to 100s of km), the horizontal distribution of plankton is dictated by large scale physical features. However, at smaller scales (1 mm to 100s of m), active swimming behavior by plankton can dominate local physical features thereby regulating patterns

of distribution (Genin et al. 2005). Our finding that *Aurelia* sp. accumulate in regions of highest vertical velocity shear suggests a behavioral response of medusae to velocity shear.

Velocity shear may develop at the air-sea interface, the benthic boundary layer or at an interface between two dissimilar water masses. Although medusae in the northern Gulf of Mexico typically experience shear that is driven by a salinity gradient (Schroeder and Wiseman 1999), the physical properties and density structure of fronts in the Gulf of Mexico are comparable to physical gradients in other areas. Boundaries between water masses are characterized by sharp gradients in salinity, temperature and velocity, and these physical interfaces often coincide with biological discontinuities including chlorophyll maxima and plankton patches (e.g., McManus et al. 2003). Zooplankters with sufficiently high swimming speeds are capable of overcoming local flow (Yamazaki and Squires 1996) and forming layers at shear interfaces (Gallager et al. 2004). During this study, groups of medusae were abundant in areas with relatively high velocity shear often associated with the pycnocline (Figs. 2-4).

While the precise sensory mechanism behind orienting to shear remains unresolved, laboratory investigations provide evidence that a medusae can maintain a position into a velocity gradient by maintaining a higher overall bell margin angle on the side of the bell in higher flow velocity (Table 2; Fig. 11). This behavior bears a resemblance to the turning mechanics of scyphomedusae described by Gladfelter (1972, 1973). During turning in scyphomedusae, Gladfelter described unilateral swimming in which a contraction was initiated on one side (i.e., the inboard side) of the bell and after a delay, the lagging side (outboard side) contracted at a greater rate. The angle of contraction was always higher on the initiating side but this was only due to its initial lead.

The difference in phase shift between the two sides of the bell (Table 3; Fig. 11), confirmed that medusae swimming in shear initiated contractions on the lower flow side of the bell. The low flow side of the bell contracted more strongly, while the higher flow side of the bell maintained a higher angle throughout a pulse cycle (Fig. 11). At any given time the more contracted side was on the low flow side (inboard), so when the outboard side contracted, a thrust was produced that shifted the umbrellar axis and counteracted the rotational force produced by the velocity gradient.

Despite the difference in angle between the two sides of the bell, the amplitude was the same indicating that the overall magnitude of contraction did not differ between sides (Table 3). Additionally, the contraction period was the same between sides of the bell, which could be predicted based on the neural circuitry of cnidarians (Table 3). Conduction of impulses is all-or-none and once a pulse is initiated, it spreads to the entire bell. So, although it is possible for contraction to be delayed on one side of the bell, it is unlikely that one side could pulse at a different frequency than the other. On the whole, the behavior that a medusa employs to counteract the rotational force imposed by a velocity gradient is the same behavior exhibited by turning medusae.

The observation that groups of medusae orient to flow implies a selective advantage to this behavior. Orienting to currents or shear regimes could serve a variety of adaptive purposes including increased prey encounter rates (Rothschild and Osborn 1988), increased fertilization success (Higgins 2005) and refuge from damaging levels of shear and turbulence, that may differ between taxa and even between populations of the same species depending on local, ecological conditions (Hamner 1995; Dawson and Hamner 2003). By orienting to a current,

scyphomedusae may increase prey contact rates by spending more time in regions where fluid velocity, prey abundance and prey diversity are optimal.

References

Batschelet, E. 1981. Circular statistics in biology, Academic Press.

Budelmann, B. 1988. Morphological diversity of equilibrium receptor systems in aquatic invertebrates. *In* J. Attema [ed.], Sensory Biology of Aquatic Animals. Springer-Verlag.

Costello, J. H., E. Klos, and M. D. Ford. 1998. In situ time budgets of the scyphomedusae *Aurelia aurita*, *Cyanea* sp., and *Chrysaora quinquecirrha*. J. Plankton Res. **20:** 383-391.

Cowan, J. H., and E. D. Houde. 1993. Relative predation potentials of scyphomedusae, ctenophores and planktivorous fish on ichthyoplankton in Chesapeake Bay. Mar. Ecol. Prog. Ser. **95:** 55-65.

Dawson, M. N., and W. M. Hamner. 2003. Geographic variation and behavioral evolution in marine plankton: The case of *Mastigias* (Scyphozoa, Rhizostomeae). Mar. Biol. **143:** 1161-1174.

Gallager, S. M., H. Yamazaki, and C. S. Davis. 2004. Contribution of fine-scale vertical structure and swimming behavior to formation of plankton layers on Georges Bank. Mar. Ecol. Prog. Ser. **267:** 27-43.

Genin, A., J. S. Jaffe, R. Reef, C. Richter, and P. J. S. Franks. 2005. Swimming against the flow: a mechanism of zooplankton aggregation. Science. **308:** 860-862.

Gladfelter, W. B. 1973. A comparative analysis of the locomotory systems of medusoid cnidaria. Hegoland. wiss. Meer. **25:** 228-272.

Gladfelter, W. B. 1972. Structure and function of the locomotory system of the Scyphomedusa *Cyanea capillata*. Mar. Biol. **14:** 150-160.

Graham, W. M. 2001. Numerical increases and distributional shifts of *Chrysaora quinquecirrha* (Desor) and *Aurelia aurita* (Linne) (Cnidaria: Scyphozoa) in the northern Gulf of Mexico. Hydrobiologia **451:** 97-111.

Graham, W. M. 1994. The physical oceanography and ecology of upwelling shadows. Ph.D. thesis. Univ. of California, Santa Cruz.

Graham, W. M., D. L. Martin, D. L. Felder, V. L. Asper, and H. M. Perry. 2003a. Ecological and economic implications of a tropical jellyfish invader in the Gulf of Mexico. Biological Invasions **5:** 53-69.

Graham W.M., D. L. Martin, and J. C. Martin. 2003b. In situ quantification and analysis of large jellyfish using a novel video profiler. Mar. Ecol. Prog. Ser. **254:** 129-140.

Graham, W. M., F. Pages, and W. M. Hamner. 2001. A physical context for gelatinous zooplankton aggregations: A review. Hydrobiologia **451:** 199-212.

Hamner, W. M. 1995. Sensory ecology of scyphomedusae. Mar. Freshw. Behav. Physiol. **26:** 101-118.

Hamner, W. M. 1990. Design developments in the planktonkreisel, a plankton aquarium for ships at sea. J. Plankton Res. **12:** 397-400.

Hamner, W. M., and D. Schneider. 1986. Regularly spaced rows of medusae in the Bering Sea: Role of Langmuir circulation. Limnol. Oceanogr. **31:** 171-177.

Higgins, J. E. 2005. Overcoming gamete dilution in free-spawning zooplankton: How the moon jellyfish, Aurelia sp., exploits the water column to maximize fertilization success. Ph.D. thesis. Univ. S. Alabama.

Hündgen, M., and C. Biela. 1982. Fine structure touch-plates in the scyphomedusan *Aurelia aurita*. Journal of Ultrastructure Research **80:** 178-184.

Liermann, M., A. Steel, M. Rosing, and P. Guttorp. 2004. Random denominators and the analysis of ratio data. Environ. Ecol. Stat. **11:** 55-71.

Mackas, D. L., K. L. Denman, and M. R. Abott. 1985. Plankton patchiness: Biology in the physical vernacular. Bull. Mar. Sci. **37:** 652-674.

Mackie, G. O. 1999. Coelenterate organs. Mar. Fresh. Behav. Physiol. **32:** 113-127.

McManus, M. A., A. L. Alldredge, A. H. Barnard, E. Boss, J. F. Case, T. J. Cowles, P. L. Donaghay, L. B. Eisner, D. J. Gifford, C. F. Greenlaw, C. M. Herren, D. V. Holliday, D. Johnson, S. MacIntyre, D.M. McGehee, T. R. Osborn, M. J. Perry, R. E. Pieper, J. E. B. Rines, D. C. Smith, J. M. Sullivan, M. K. Talbot, M. S. Twardowski, A. Weidemann, J. R. Zaneveld. 2003. Characteristics, distribution and persistence of thin layers over a 48 hour period. Mar. Ecol. Prog. Ser. **261:** 1-19.

Nielson, A. S., A. W. Pedson, and H. R. Riisgard. 1997. Implications of density driven currents for interaction between jellyfish (*Aurelia aurita*) and zooplankton in a Danish fjord. Sarsia **82:** 297-305.

Purcell, J. E., and M. N. Arai 2001. Interactions of pelagic cnidarians and ctenophores and fish: A review. Hydrobiologia **451:** 27-44.

Raskoff, K. A., F. A. Sommer, W. M. Hamner, and K. M. Cross. 2003. Collection and culture techniques for gelatinous zooplankton. Biol. Bull. **204:** 68-80.

Rothschild, B. J., and T. R. Osborn. 1988. Small-scale turbulence and plankton contact rates. J. Plankton Res. **10:** 465-474.

Schroeder, W. W., and W. J. Wiseman. 1999. Geology and hydrodynamics of Gulf of Mexico estuaries. p. 3-22. *In* T. S. Bianchi, J. R. Pennock and R. R. Twilley [eds.], Biogeochemistry of Gulf of Mexico estuaries. John Wiley & Sons, Inc.

Shanks, A. L., and W. M. Graham. 1987. Oriented swimming in the jellyfish *Stomolophus meleagris* L. Aggassiz (Scyphozoa: Rhizostomida). J. exp. mar. Biol. Ecol. **108:** 150-169.

Sparks, C., E. Buecher, A. S. Brierly, B. E. Axelson, H. Boyer, and M. J. Gibbons. 2001. Observations on the distribution and relative abundance of the scyphomedusan *Chrysaora hyoscella* (Linne, 1766) and the hydrozoan *Aequorea aeqourea* (Forskal, 1775) in the northern Benguela ecosystem. Hydrobiologia **451:** 275-286.

Sullivan, B. K., D. Van Keuren, and M. Clancy. 2001. Timing and size of blooms of the ctenophore, Mnemiopsis leidyi in relation to temperature in Naragansett Bay, RI. Hydrobiologia **451:** 113-120.

Tiselius, P., G. Nielson, and T. G. Nielson. 1994. Microscale patchiness of plankton within a sharp pycnocline. J. Plankton Res. **16:** 543-554.

Yamazaki, H., and K. D. Squires. 1996. Comparison of oceanic turbulence and copepod swimming. Mar. Ecol. Prog. Ser. **144:** 299-301.

Table 1. Vertical velocity (mean ± standard error of the mean) and shear values from horizontal transects at each flow treatment in pseudokreisel. Positive velocities are upward.

| Horizontal distance (cm) | Velocity (cm $s^{-1}$) | Shear ($s^{-1}$) | Velocity (cm $s^{-1}$) | Shear ($s^{-1}$) | Velocity (cm $s^{-1}$) | Shear ($s^{-1}$) |
|---|---|---|---|---|---|---|
| 0 | 3.02 ± 0.28 | | 6.10 ± 0.35 | | 10.21 ± 0.05 | |
| 5 | 2.48 ± 0.77 | 0.11 | 4.32 ± 0.59 | 0.36 | 7.99 ± 0.08 | 0.44 |
| 10 | 1.60 ± 0.16 | 0.18 | 2.90 ± 0.36 | 0.28 | 5.65 ± 0.05 | 0.47 |
| 15 | 1.05 ± 0.06 | 0.11 | 1.79 ± 0.26 | 0.22 | 3.10 ± 0.33 | 0.51 |
| 20 | 0.40 ± 0.09 | 0.13 | 1.05 ± 0.18 | 0.15 | 1.69 ± 0.1 | 0.28 |
| 25 | 0.20 ± 0.07 | 0.04 | 0.19 ± 0.07 | 0.17 | 0.86 ± 0.1 | 0.16 |
| 30 | -0.07 ± 0.1 | 0.05 | -0.06 ± 0.16 | 0.05 | -0.12 ± 0.37 | 0.20 |
| Means: | 1.24 | 0.10 | 2.33 | 0.21 | 4.20 | 0.34 |

Table 2. Low vs. high flow sides of bell margin angle means (two-sample *t*-test).

| Treatment ($s^{-1}$) | *n* | High angle (rad) | Low angle (rad) | *p*-value |
|---|---|---|---|---|
| no flow | 8 | 0.97 | 0.99 | 0.77 |
| 0.1 | 10 | 0.99 | 0.94 | 0.35 |
| 0.21 | 9 | 0.94 | 0.89 | 0.25 |
| 0.34 | 10 | 1.02 | 0.94 | 0.05 |

Table 3. Model parameter coefficient means for low vs. high flow sides of bell in no flow and 0.34 $s^{-1}$ shear treatments.

No flow
$n$=8

| Parameters | | High flow | Low flow | $p$ - value |
|---|---|---|---|---|
| Amplitude (rad) | $a$ | 0.19 | 0.19 | 0.97 |
| Period (s) | $b$ | 2.62 | 2.63 | 0.97 |
| Phase shift (s) | $c$ | 2.80 | 2.78 | 0.98 |
| Vertical offset (rad) | $y_o$ | 0.97 | 0.98 | 0.88 |

Shear rate = 0.34 $s^{-1}$
$n$=10

| Parameters | | High flow | Low flow | $p$ - value |
|---|---|---|---|---|
| Amplitude (rad) | $a$ | 0.22 | 0.22 | 0.80 |
| Period (s) | $b$ | 2.36 | 2.38 | 0.92 |
| Phase shift (s) | $c$ | 2.00 | 2.20 | 0.70 |
| Vertical offset (rad) | $y_o$ | 1.02 | 0.95 | 0.05* |

Table 4. Differences in phase shift, *c*, between low flow and high flow bell margin angles for each treatment.

| | Phase shift | | |
|---|---|---|---|
| Flow treatment ($s^{-1}$) | High flow (s) | Low flow (s) | Difference in phase shift (s) |
| No flow | 2.80 | 2.78 | -0.02 |
| Low | 2.93 | 3.01 | 0.08 |
| Medium | 1.75 | 1.86 | 0.11 |
| High | 2.00 | 2.20 | 0.20 |

Fig. 1. *Aurelia* sp. morphology and landmarks used for swimming measurements. Margin angles in high flow ($\Phi_h$) and low flow ($\Phi_l$) are expressed in degrees relative to the heading of the medusa ($\theta$). (A) Side view. (B) Aboral view.

Fig. 2. Vertical profiles of *Aurelia* sp. distribution and physical structure on 13 August 2000. Gray shading highlights regions of shear. (A) Vertical profiles of density and current velocity (mean ± SE over 1 min) (B) Vertical distribution of *Aurelia* sp. with density profile. (C) Circular frequency histograms of *Aurelia* sp. swimming orientation. Concentric circles correspond to numbers of individuals observed, $\Phi$ is the mean swimming direction, *z* is Rayleigh's test statistic, *p* is the significance level and *n* is the number jellyfish observed.

Fig. 3. *Aurelia* sp. swimming orientation during cast taken 18 August 2000. Gray shading highlights regions of shear. Shearing in benthic boundary layer not based on measured velocity values. Panels as in Fig. 2.

Fig. 4. *Aurelia* sp. swimming orientation during cast taken 29 August 2000. Panels as in Fig. 2.

Fig. 5. Flow vector field in pseudokreisel tank at shear rate of 0.21 $s^{-1}$. Black square indicates area where behavioral observations were made. Vector legend is shown in bottom right corner.

Fig. 6. Distribution of vertical velocity (bars are standard error of the mean) and shear taken along a horizontal transect in pseudokreisel. Positive velocities are upward.

Fig. 7. Video frame sequence of *Aurelia* sp. swimming in shear a shear velocity of 0.34 $s^{-1}$. The pulse is initiated on the lower flow side of the bell (right side) and a higher bell margin angle is maintained on the low flow side of the bell.

Fig. 8. Representative plots of jellyfish swimming in varying flow fields (A) no flow and (B) a shear velocity 0.34 $s^{-1}$. Peaks correspond to maximum relaxation and troughs correspond to fullest contraction.

Fig. 9. *Aurelia* sp. bell angle ratios for four shear treatments. Means with same letters are not significantly different at $p<0.05$. Theoretical balanced swimming is indicated by dashed line (1:1). Box boundaries are $25^{th}$ and $75^{th}$ percentiles and error bars are $90^{th}$ and $10^{th}$ percentiles. Thin line is the median and thicker line is the mean.

Fig. 10. General four parameter sine curve. $y_o$ is the height of the baseline or average angle, $a$ is the amplitude or half of the angular range, $b$ is the period, and $c$ is the phase shift or temporal offset.

Fig. 11. Typical waveforms of *Aurelia* sp. swimming as derived from mean equation parameters. A –D are plotted equations for the low and high flow sides of the bell margin angle and correspond to shear treatments of no flow, 0.1, 0.21, and 0.34 $s^{-1}$ respectively. E- H are corresponding ratios of low flow to high flow bell margin angles. Dashed lines represent time-averaged means.

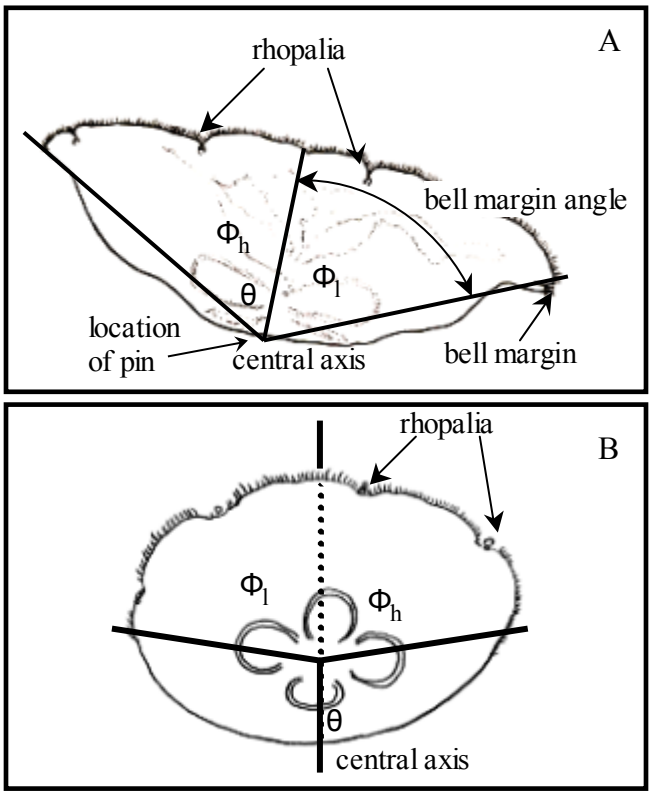


Rakow & Graham Fig. 1

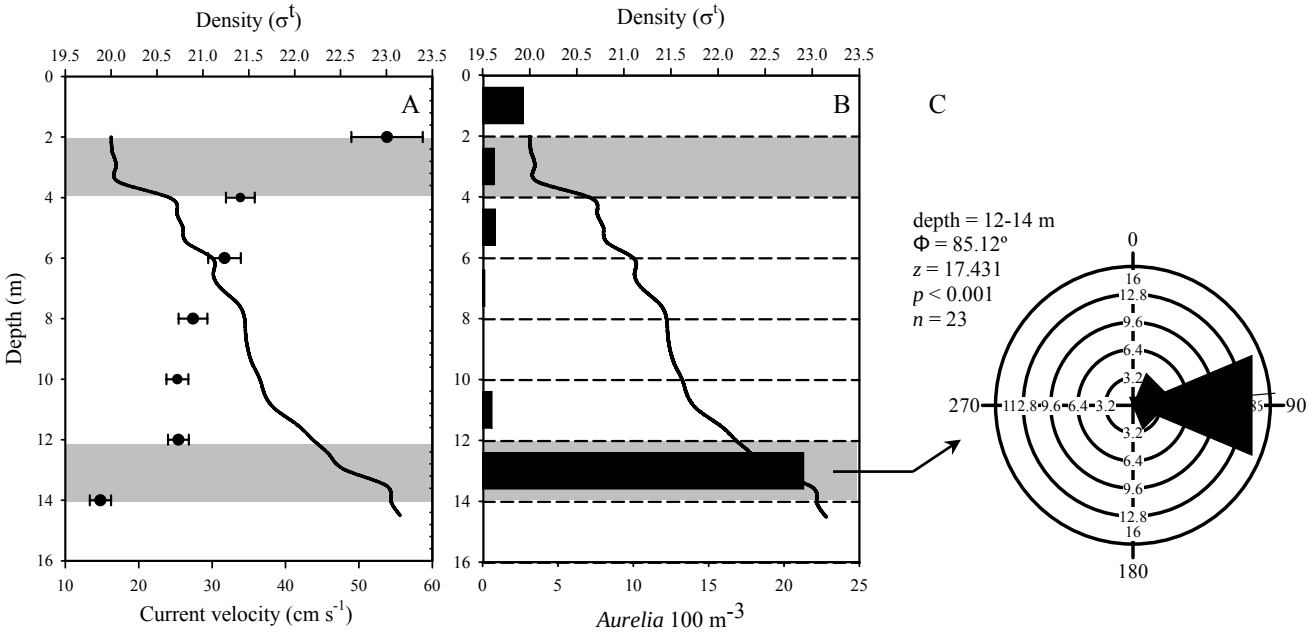


Rakow & Graham Fig. 2

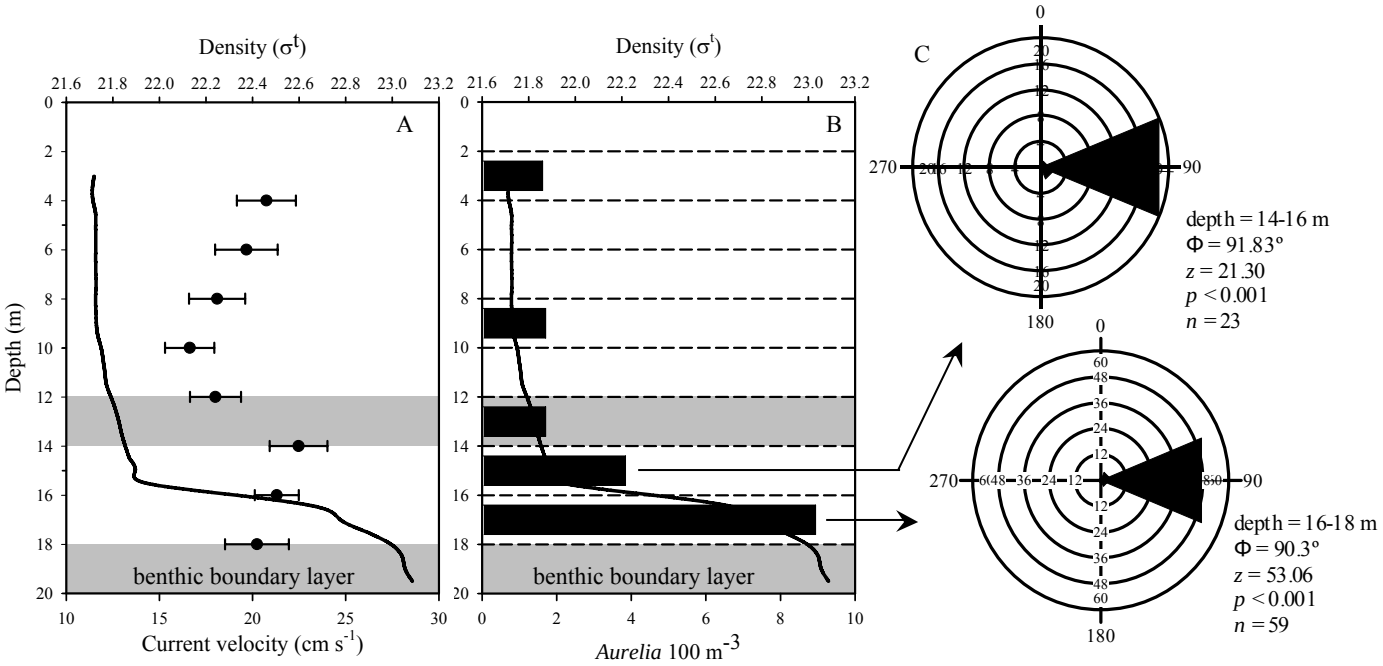


Rakow & Graham Fig. 3

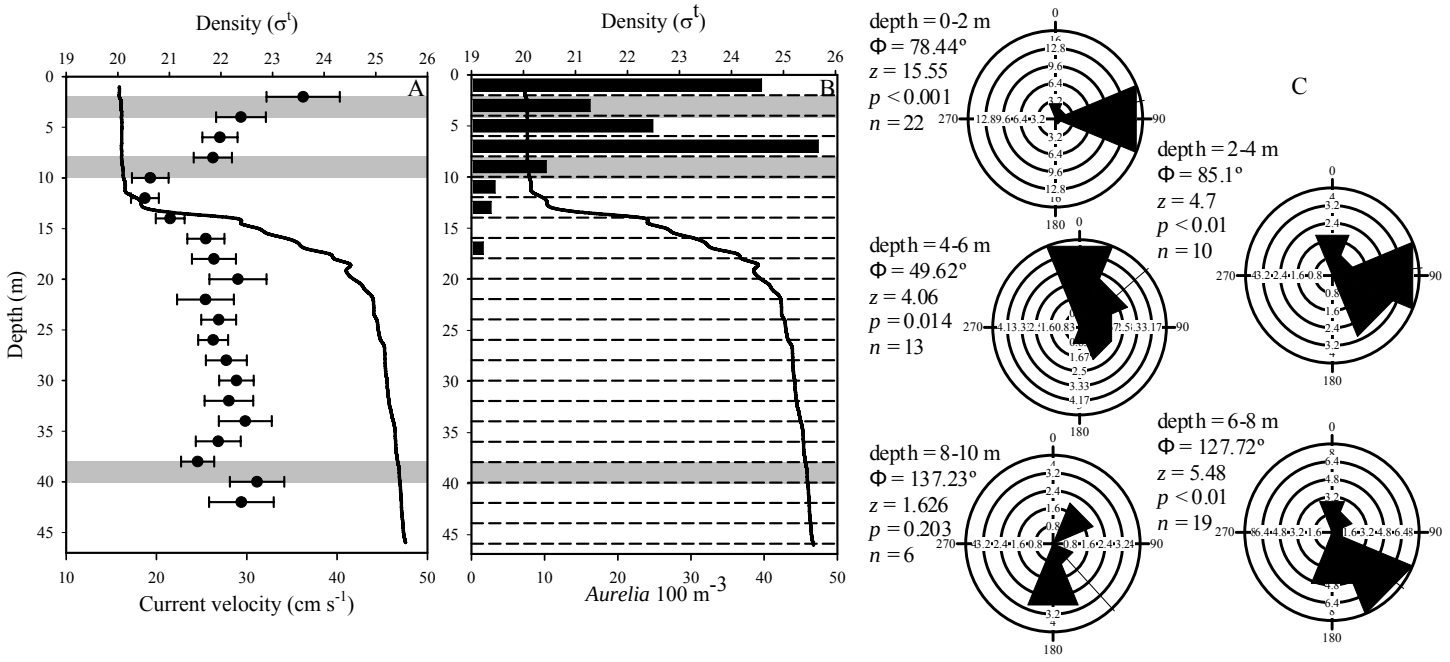


Rakow & Graham Fig. 4

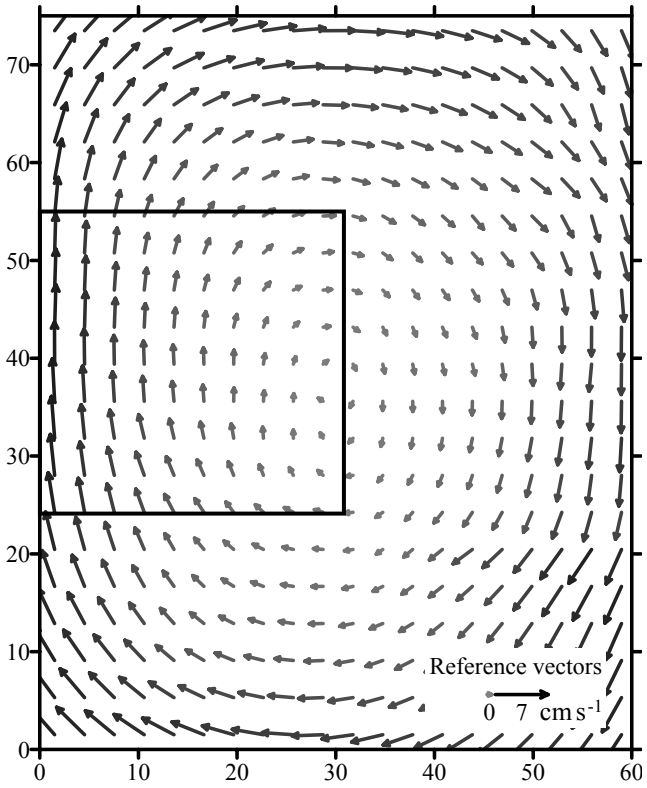


Rakow & Graham Fig. 5

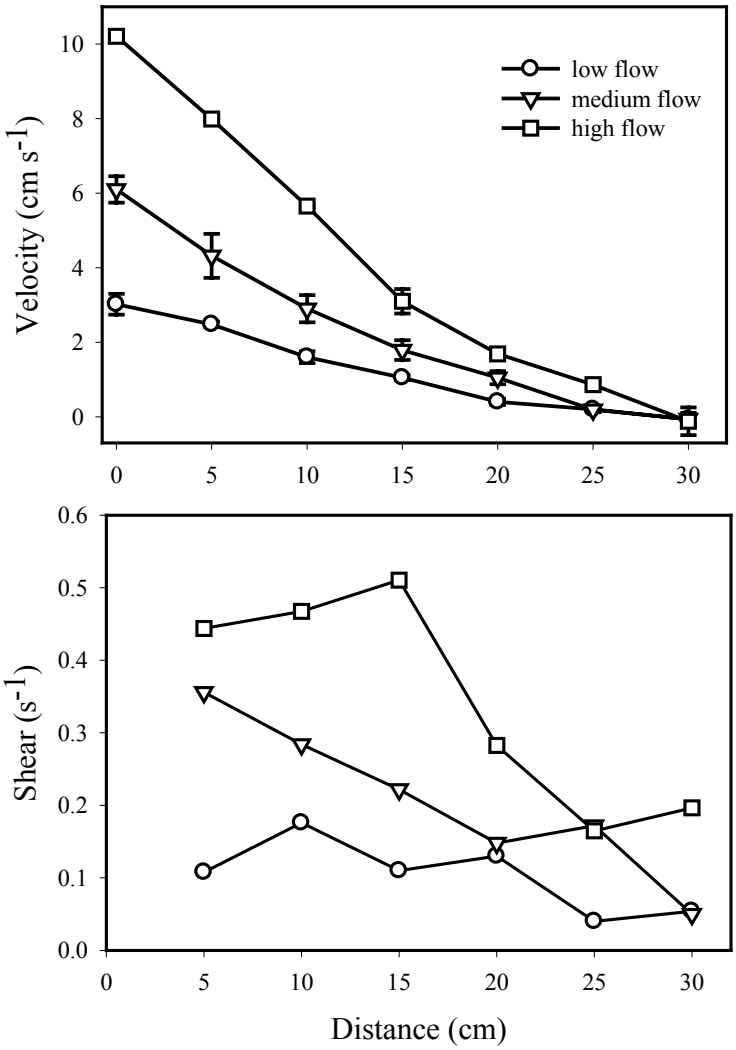


Rakow & Graham Fig. 6

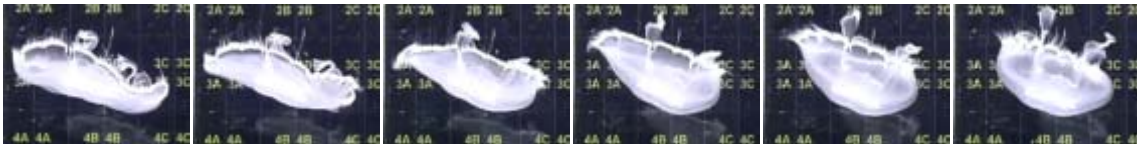

Rakow & Graham Fig. 7

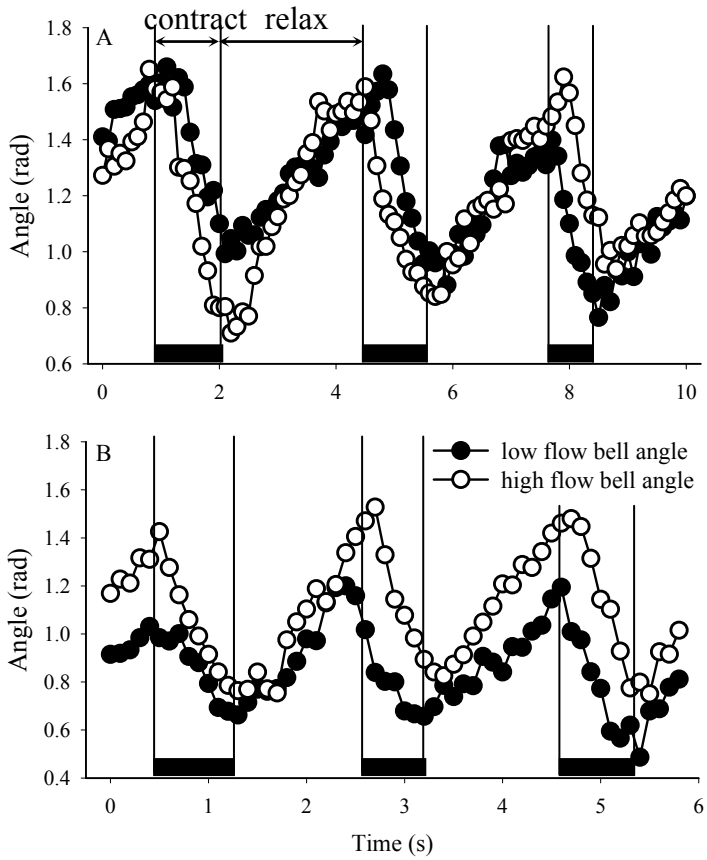


Rakow & Graham Fig. 8

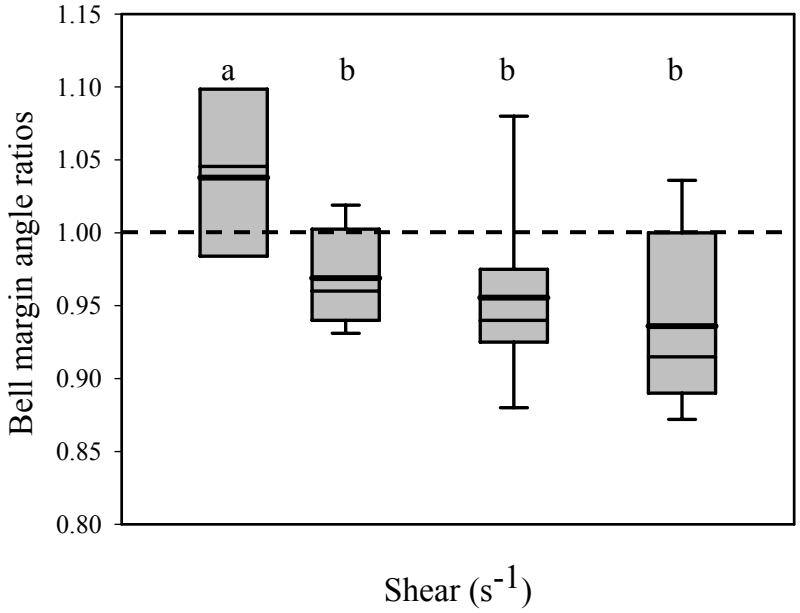


Rakow & Graham Fig. 9

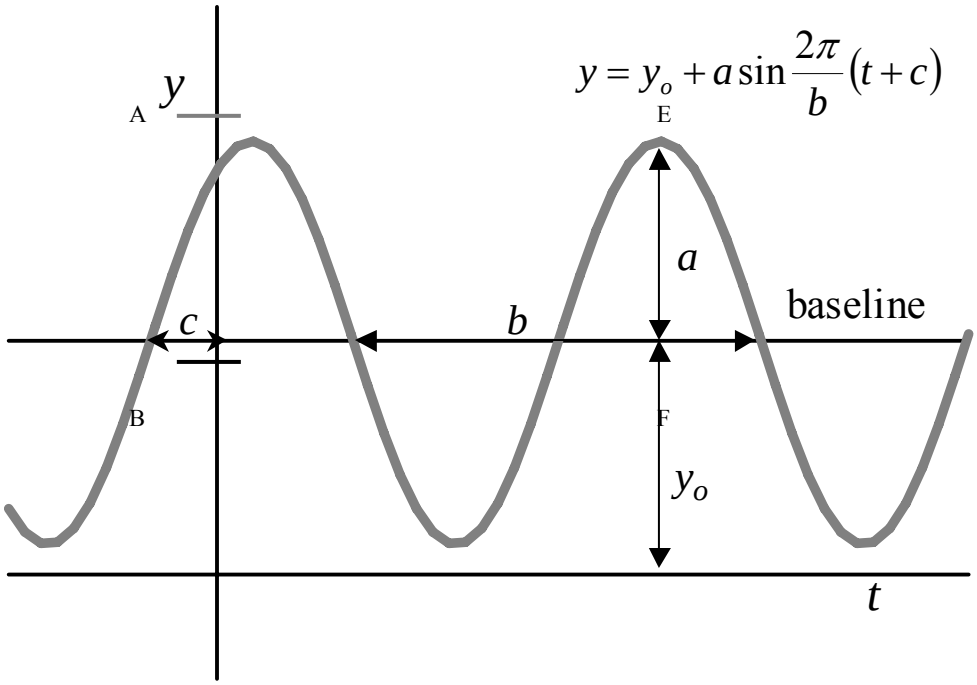


Rakow & Graham Fig. 10

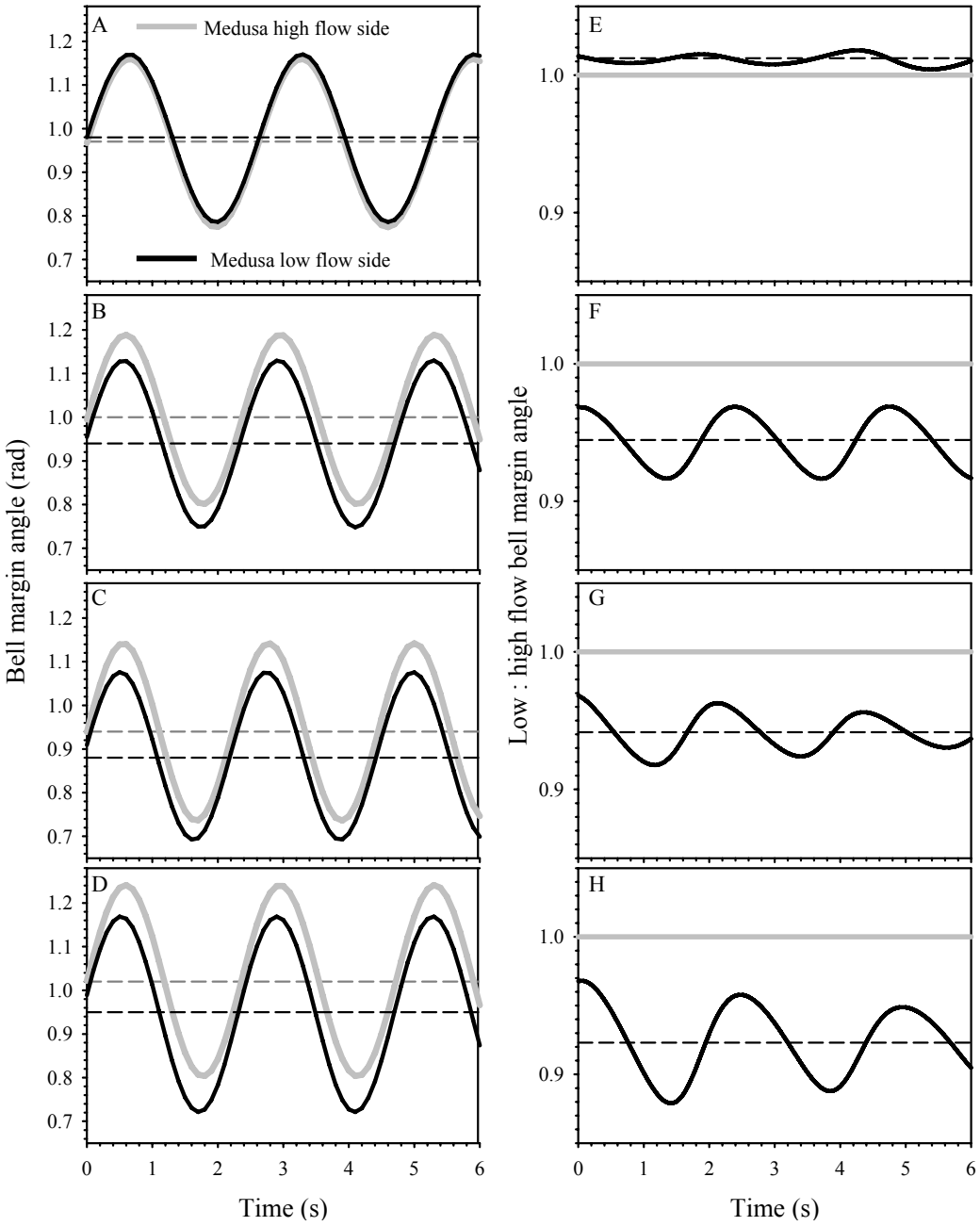


Rakow & Graham Fig. 11